Subchannel and Computational Fluid Dynamic Analyses of a Model Pin Bundle

A. Gairola[a], M. Arif[a], K.Y. Suh[a,b]*
[a]*Department of Nuclear Engineering, Seoul National University, 1 Gwanak Ro, Gwanak Gu, Seoul 151-744, ROK*
[b]*PhiloSophia Inc., 1 Gwanak Ro, Gwanak Gu, Seoul 151-744, ROK*
Corresponding author: kysuh@snu.ac.kr

1. Introduction

In the framework of the 11th international meeting of International Association for Hydraulic Research and Engineering (IAHR) working group on the advanced reactor thermal hydraulics a standard problem was conducted. The quintessence of the problem was to check on the hydraulics and heat transfer in a novel pin bundle with different pitch to rod diameter ratio and heat flux cooled by liquid metal. The standard problem stems from the field of nuclear safety research with the idea of validating and checking the performances of computer codes against the experimental results. Comprehensive checks between the two will succor in improving the dependability and exactness of the codes used for accident simulations.

2. Details of Model Assembly and Experiment

2.1Model Assembly

The model subassembly of the BREST type reactor (Fig. 1and Table I) is chosen for the experimental setup. In this 25 pins were housed in a square rapper with different pitch to diameter ratio (s/d_1 = 1.25 and s/d_2 = 1.46) and heat flux. This arrangement of pins was mounted in a cylindrical vessel held by top and bottom centering spacers and held in the middle by a transverse spacer located at 372 mm from the initial point of heat production. The heated length of 960 mm is cooled by an eutectic alloy sodium-potassium (22% Na+78% K).

In the middle of the square array there was a rotating measuring pin simulator used for temperature measurement of the heat exchange surface (Fig. 2). On its surface there were 12 micro thermocouples jammed in longitudinal grooves and arranged in an azimuthal step size of 30°.The coolant temperature was measured at the exit of the pin bundle using micro thermocouples. Non measuring pins are immovable and were electrically heated using nichrome heating elements arranged in a spiral fashion providing constant heat flux over the height and perimeter of the simulator.

An important element of the assembly is spacer grid. It is essentially a frame which is made up of plates (1.2 mm thick) inserted one into another. The smooth pin simulators were held tightly by the sills protruding out of the cells made by the plates (thickness of plates from which sills were executed is 0.3 mm).

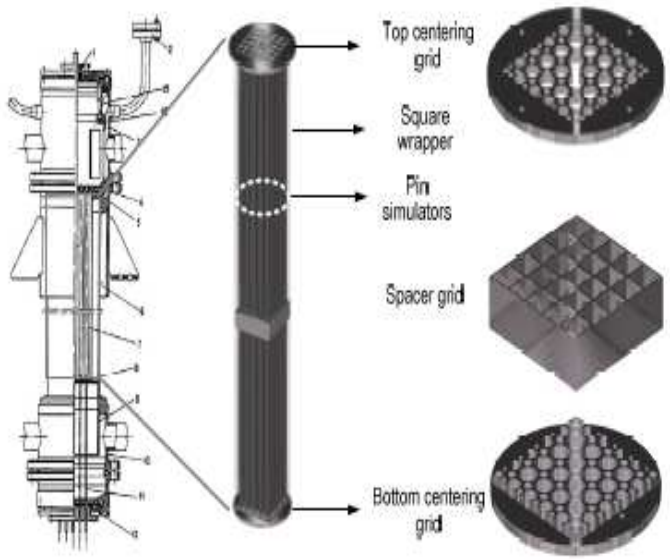

Fig. 1. Test bundle

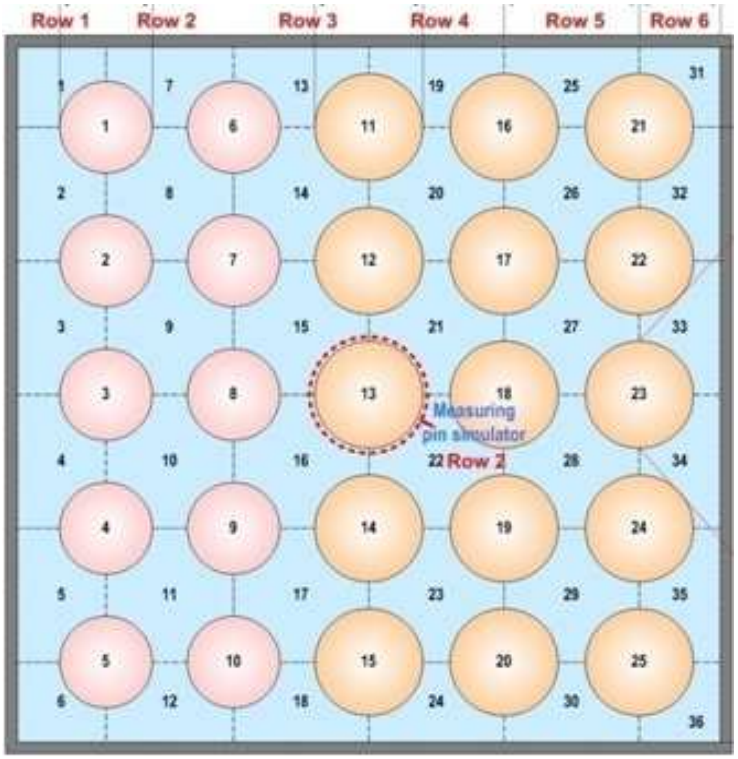

Fig. 2. Cross section of pin simulator

Table I: Main Parameters for the Model Bundle

Parameters	Zone of the bundle	
Outer pin diameter (mm)	14	12
Number of pin simulator	15	10
Pitch to diameter ratio (s/d)	1.25	1.46
Length of pin simulator (mm)	1014	
Heated Length (mm)	960	

2.2 Experiment

In this experiment surface temperature of the simulator and the coolant temperature was recorded. In addition to it hydrodynamic studies were performed using electromagnetic measurement techniques. Velocity profile around the central pin simulator was measured as it is the inflexion point for the diametrical change. Special attention was given to the changes in the flow induced by the spacer grids.

Three Experiments were performed with five different input temperatures and by varying the pin power ratio.

The calculated Reynolds number for the assembly was 53393. It was calculated from the equation

$$\overline{\mathrm{Re}} = \frac{\overline{w} d_h}{v}$$

where $\overline{w}$ is the mean velocity calculated by area averaging the coolant flow rate. The coolant flow rate is measured using electromagnetic technique and was given by the equation, V=4.55 E (m^3/h) where E is the EMF.

3. Subchannel Analysis

This is performed by using MATRA (Multi Channel Analyzer for Transient and steady state in Rod Arrays). A subchannel analysis approach is used for increasing the predictive capabilities of the code with reasonable computing time. Essentially this approach divides the flow area into many channels and each subchannel is further divided into control volumes. Conservation equations were solved for the subchannels and a 3-D picture is presented by combining the various control volumes.

The equations used by MATRA follow.

$$A\frac{\partial \rho}{\partial t} + \frac{\partial m}{\partial x} + [DC]^T \omega = 0 ...(1)$$

$$A\frac{\partial \rho h}{\partial t} + \frac{\partial mh}{\partial x} + [DC]^T h^* \omega = q ...(2)'$$

$$\frac{\partial m}{\partial t} + \frac{\partial mh}{\partial x} + [DC]^T u^* \omega + A\frac{dp}{dx} = F ...(3)$$

$$\frac{\partial \omega}{\partial t} + \frac{\partial u^* \omega}{\partial x} + \frac{\partial v_y \omega^*}{\partial y} - [DC]P = C ...(4)$$

They are essentially the continuity, energy and momentum equations respectively. The last two are the axial and transverse momentum equations.

4. MATRA Calculations

A very simple hand calculation was performed before running the MATRA simulation. In this calculation it was assumed that there is no momentum or energy transferred between the different subchannels. Thus simply integrating the linear power density over the length of the channel

$$q'(z)dz = mdh = mc_p dt ...(5)$$

$\Delta T = \frac{Q}{mc_p} ...(6)$, which is the temperature rise of the coolant per channel.

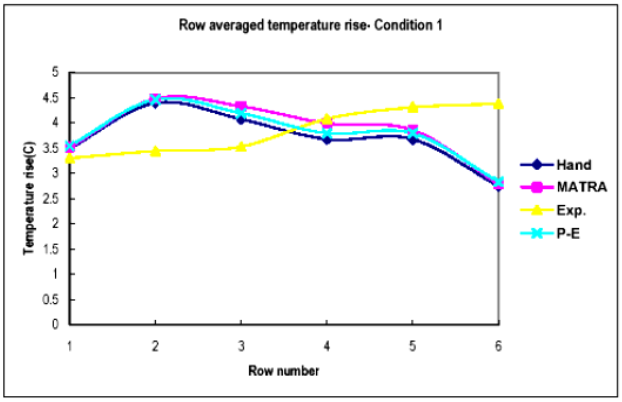

Fig. 3. MATRA calculation at inlet temperature of 55.84°C.

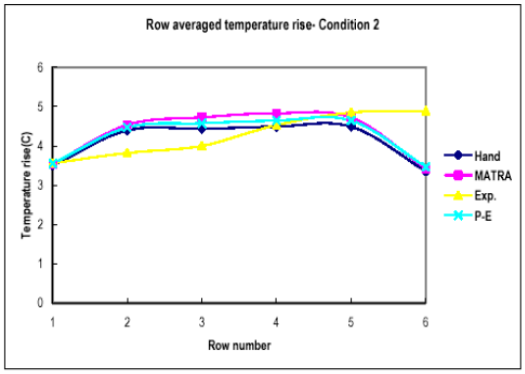

Fig. 4. MATRA calculation at inlet temperature of 59.21°C.

The hand calculation results are very similar to the MATRA calculations. However, the MATRA and the hand calculations results deviate from the experimental data. The test revealed that the highest temperature rise is in the row near the edge of the wrapper and it varies strongly after the inflexion point of the diameter. Results of hand calculations are a little lower than MATRA as the turbulent mixing induced by the grid spacer is not considered in hand calculations. However the MATRA results are not excellent either as the transverse momentum equation used in MATRA is unable to define the situation perfectly; predicting lower values on the edge and higher values in the middle.

5. CFD Simulation with Detailed Geometry of the Grid Spacer

The ANSYS-CFX computational fluid dynamic (CFD) code is used for this simulation while incorporating a detailed geometry for the grid spacer. ANSYS-CFX utilizes finite volume method approach to solve the Navier Stokes equation in the conservative form. The Navier Stokes equation in conservative form is essentially written for a control volume fixed in space.

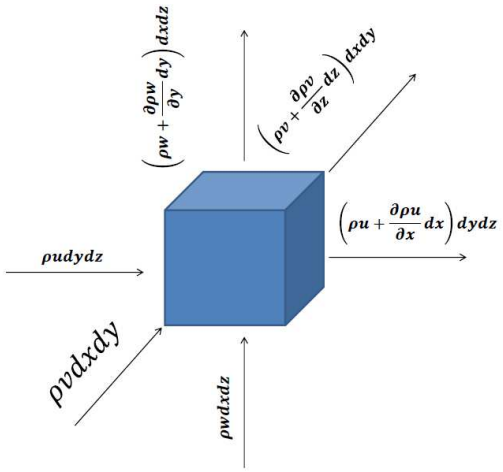

Fig. 5. Continuity equation.

The scheme is shown for the continuity equation in Fig. 5.

The conservative forms of continuity, momentum and energy follow.

Continuity:

$$\frac{\partial \rho}{\partial t} + \nabla \cdot \rho U = 0 ...(7)$$

Momentum:

$$\frac{\partial (\rho \mathrm{U})}{\partial t} + \nabla \cdot (\rho U \otimes U) = -\nabla p + \nabla \tau + S_M ...(8)$$

$$\tau = \mu(\nabla U + (\nabla U)^T - \frac{2}{3}\delta \nabla \cdot U) ...(9)$$

(Stress tensor and strain rate relation)

Energy:

$$\frac{\partial (\rho h_{tot})}{\partial t} - \frac{\partial p}{\partial t} + \nabla \cdot (\rho U h_{tot}) = \nabla \cdot (\lambda \nabla T) + \nabla \cdot (U \cdot \tau) + \mathrm{U} \cdot \mathrm{S}_M + S_E ...(10)$$

Where h_{tot} is the stagnation enthalpy, the last two terms in the above equation are the viscous work term and the work due to external momentum sources To accurately capture the effect of grid spacer a detailed computer aided design (CAD) geometry was input to the CFD simulation.

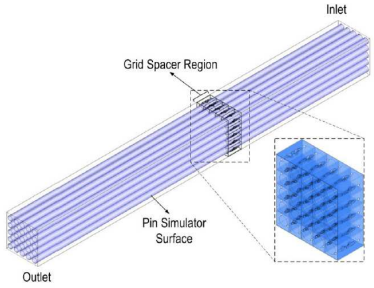

Fig. 6. Model pin bundle computational domain.

However, the effect of turbulence is to be predicted by using suitable turbulence model, which is a complex process as is unsteady and consists of many scales.

To model the effect of turbulence the Navier Stokes equation are modified to RANS (Reynolds Averaged Navier Stokes) with an average and fluctuating component of velocity.

$$U = \overline{U_i} + u_i ...(11)$$

Where the first term on the right hand side is the average component of velocity and the other is fluctuating component. This leads to continuity equation which is similar to original; however the momentum and

energy terms are modified. This modification introduces an additional stress term in the momentum equation which is known as Reynolds stress and is given by $\rho\overline{u_i u_j}(12)$. Thus introducing additional convective terms arising because of fluctuations in the velocity and which will enhance mixing effect. Similarly for the energy equation the total enthalpy is modified as

$$h_{tot} = h + \frac{1}{2}U_i U_i + k ...(13)$$

$$k = \frac{1}{2}\overline{u_i^2} ...(14)$$

The last term is the turbulent kinetic energy.

In eddy viscosity model the Reynolds stress is proportional to the mean velocity gradient and eddy viscosity terms.

In the $K-\omega$ turbulence model eddy viscosity is directly proportional to turbulent kinetic energy and inversely to turbulent frequency (omega). This model is better performing and converge stably, thus it was used during the simulation.

While simulating the flow in the model bundle finer mesh structure is used near the pin surface to accurately evaluate the boundary layer of the fluid. Quadrilateral elements are used for meshing except near the grid spacer region to reduce the amount of computational efforts. Also the size of the first mesh is kept limited to 30 as not to surpass the boundary layer region and to produce erroneous results.

Given the boundary conditions in table II the following results were obtained and compared against a past simulation in which the geometry of the grid spacer was less accurately captured in the CAD drawing.

Table II: Boundary Conditions

Parameters	Values
Inlet Temperature (K)	328.99
Inlet Velocity (m/s)	2.6
Pin Power$_{15}$ (KW)	1.35
Pin Power$_{12}$ (KW)	2
Reynolds Number	53393

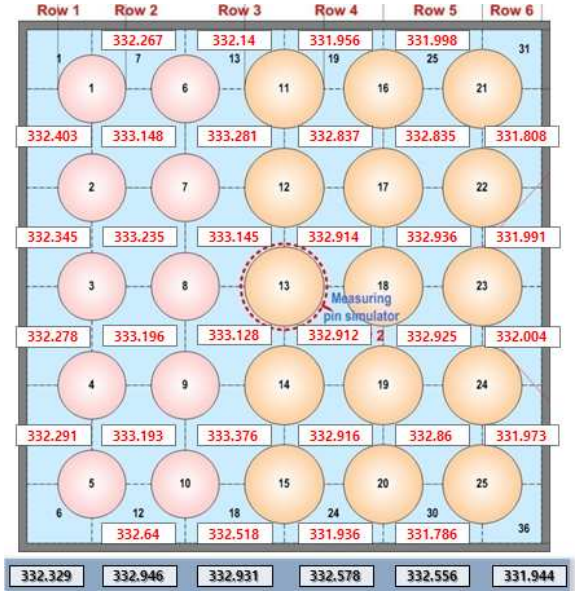

Row 1	Row 2	Row 3	Row 4	Row 5	Row 6
	332.267	332.14	331.956	331.998	
332.403	333.148	333.281	332.837	332.835	331.808
332.345	333.235	333.145	332.914	332.936	331.991
332.278	333.196	333.128	332.912	332.925	332.004
332.291	333.193	333.376	332.916	332.86	331.973
	332.64	332.518	331.936	331.786	
332.329	332.947	332.931	332.579	332.557	331.944
3.33925	3.9565	3.94133	3.5885	3.56667	2.954

Fig. 7. Average temperature.

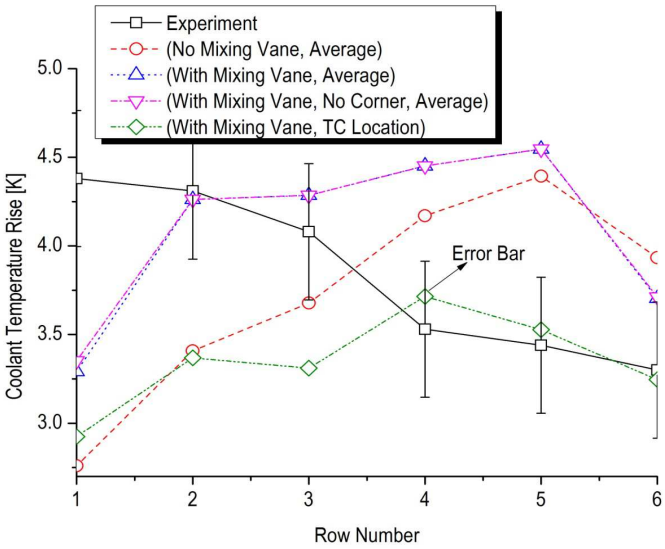

Fig. 8. Results of CFX simulation.

From the above figure (Fig. 8) It is clear that the detailed CAD drawing of the grid spacer is capturing the mixing effect better with a better prediction of the coolant exit temperature; however the results are still far from being accurate. Average temperature realization in the benchmark problem was not clear as the microthermocouples were located at the center or near the center of each channel and this may not represent

the average temperature of that particular channel. This conjecture is further borne on by the CFD simulation at the location of the thermocouples. The cross checks performed using the CFD code at the location of thermocouple shows significant gap with the real. Temperature measurement at the central pin simulator shows reasonable agreement with the CFD simulated data.

7. Effect of Grid Spacer

Fig. 9 clearly shows that the mixing effect is more pronounced on the side of higher pitch to diameter ratio.

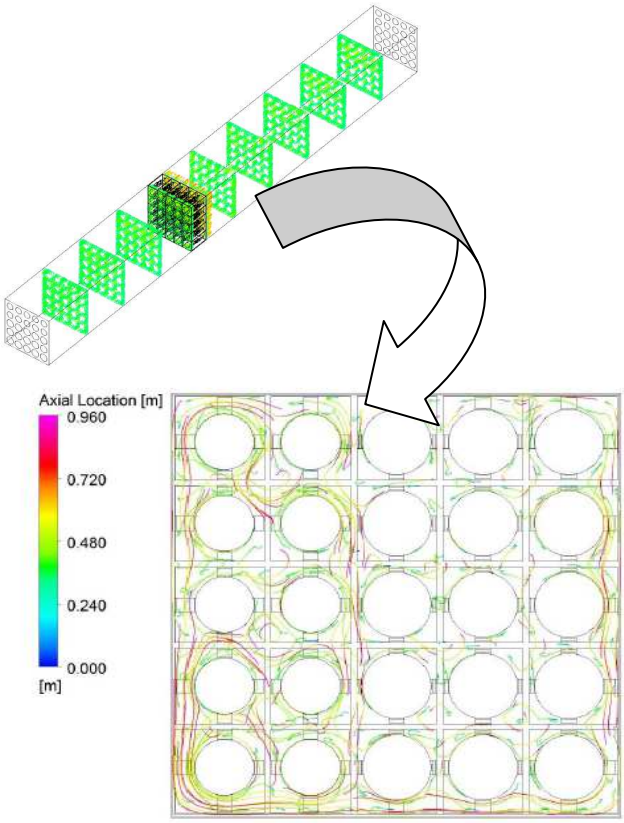

Fig. 9. Effect of grid spacer on the coolant velocity.

8. Conclusion

The current study showed that the simplistic approach of subchannel analysis code MATRA was not good in capturing the physical behavior of the coolant inside the rod bundle. With the incorporation of more detailed geometry of the grid spacer in the CFX code it was possible to approach the experimental values. However, it is vital to incorporate more advanced turbulence mixing models to more realistically simulate behavior of the liquid metal coolant inside the model pin bundle in parallel with the incorporation of the bottom and top grid structures.

ACKNOWLEDGEMENT

This work was supported by the National Research Foundation of Korea (NRF) grant funded by the Korea Government (MSIP) (No. 2008-0061900) and partly supported by the Brain Korea 21 Plus Project (No. 21A20130012821).

REFERENCES

[1] A.V. Zhukov, J.A. Kuzina, A.P. Sorokin, and G.P. Bogoslovskaia, Hydraulics And Heat Transfer In The Model Pin Bundles With Liquid Metal Coolant, International Association for Hydraulic Engineering and Research, 2003.
[2] H.M. Son and K.Y. Suh Computational Fluid Dynamic Analysis On Liquid Metal Cooled Fuel Assembly Simulator, PBNC, 2012.
[3] A.V. Zhukov et al., Hydrodynamics and Heat Transfer in Reactor Components Cooled by Liquid Metal Coolants in Single/Two-Phase, IAEA, Vienna, Austria, 2005.